KIEL-UP • DOI: 10.38072/2748-3150/p32

GOES observations of solar protons during ground level enhancements

Juan V. Rodriguez, Brian T. Kress

Correspondence
CIRES – Cooperative Institute for Research in Environmental Sciences, University of Colorado Boulder, and NCEI – National Centers for Environmental Information at NOAA – National Oceanic and Atmospheric Administration, Boulder, Colorado, USA, juan.rodriguez@noaa.gov, brian.kress@noaa.gov

Keywords
solar energetic particles; ground level enhancements; galactic cosmic rays; neutron monitor; GOES

Abstract
Since 1974, the U.S. National Oceanic and Atmospheric Administration (NOAA) has observed solar proton fluxes from the Geostationary Operational Environmental Satellites (GOES). These observations frequently have served as measurements of the primary component of ground level enhancements (GLEs). Until March 2020, when GOES-14 and -15 were turned off, solar proton measurements were made by the Energetic Particle Sensor (EPS) and the High-Energy Proton and Alpha Detector (HEPAD). EPS had poor energy resolution above 100 MeV, and NOAA derived a >100 MeV integral flux from the EPS channels to support alerts issued by the Space Weather Forecast Office. HEPAD provided some energy resolution in the 330-700 MeV range and a >700 MeV integral channel. Starting with GOES-16, a new instrument called the Solar and Galactic Proton Sensor (SGPS) has replaced EPS and HEPAD. SGPS uses three solid-state telescopes to observe solar proton fluxes between 1 and 500 MeV with a >500 MeV integral channel. The >100 MeV integral flux is now derived from SGPS observations and includes the >500 MeV flux in its derivation. In this paper, we describe the older EPS and HEPAD observations and the new SGPS solar proton observations. We also compare methods for detecting solar proton event onsets currently used with GOES and neutron monitor observations and recommend some innovations.

1. Introduction

In the study of ground level enhancements (GLEs), observations of the primary population are provided by satellite observations in Earth orbit or at the first Sun-Earth Lagrange point. One source of such observations has been the series of Geostationary Operational Environmental Satellites (GOES) operated by NOAA since 1974. The GOES series of weather satellites has operated in geostationary orbit (GEO), which most of the time lies within Earth's magnetosphere, apart from brief excursions into the magnetosheath.

KIEL-UP • DOI: 10.38072/2748-3150/p32

Access of solar energetic particles (SEPs) to GEO is affected by the geomagnetic field, more strongly at lower energies, and trapped magnetospheric proton populations are nearly always present below 2 MeV, preventing clear observations of SEPs at lower energies. However, SEP fluxes above 500 MeV, which have ground-level signatures, have unimpeded access to GEO.

The purpose of this paper is to provide an introduction to GOES observations during GLEs. These observations include the long series of Energetic Particle Sensors (EPS) and High Energy Proton and Alpha Detectors (HEPAD), which ceased operations in 2020, and the new series of Solar and Galactic Proton Sensors (SGPS), which to date have observed GLEs 72 (September 2017) and 73 (October 2021). Because the primary purpose of these space weather sensors is to support NOAA's real-time SEP event alerts, this paper compares the NOAA-issued alerts of GLEs 72 and 73 with the alerts issued by the neutron monitor-based GLE Alert Plus systems, which follow different protocols. The paper concludes with recommendations for innovations to these alert systems.

2. Detection of >100 MeV fluxes on GOES 8-15

Prior to GOES-16, SWPC issued >100 MeV proton alerts based on observations by the GOES Energetic Particle Sensor (EPS). Specifically, >100 MeV fluxes were derived from the P6 and P7 channel proton fluxes measured by the EPS Dome D5. The basic D5 design did not change from GOES-4 (launched 9 September 1980) to GOES-15 (launched 4 March 2010). It had a large fan-shaped field-of-view (70° by 130°) defined by a tungsten collimator that also shielded the sides. The outputs of two silicon surface-barrier detectors (25 mm^2, each 1500-micron thick) under an 8.0 g/cm^2 copper moderator were summed to create one energy deposition signal. The two D5 proton channels P6 and P7 were distinguished by deposited energy (P6: 3.5-28.0 MeV; P7 1.6-3.5 MeV). This relatively simple design resulted in consistent performance among the GOES 8-15 units (Rodriguez et al. 2014). However, the energy resolution was poor, and, with no anticoincidence, the observations were susceptible to contamination by protons that penetrated the structure. A copper plug on the back was penetrated by >80 MeV protons, and >120 MeV protons penetrated the tungsten collimator, resulting in a nearly omnidirectional response at the highest energies (Panametrics 1980; Sellers & Hanser 1996). The resulting energy responses were 84-200 MeV for P6 and 110-900 MeV for P7 (Onsager et al. 1996).

An algorithm developed by R. Zwickl (unpublished until documented by Rodriguez et al. 2017) estimated the >100 MeV flux by determining a piecewise power-law from the ratios of observed channel count rates. The upper integration limit of the extrapolated power law was set at 500 MeV (though P7 had a strong response to protons above 500 MeV). SWPC issued an alert when the >100 MeV flux reached 1 p/(cm^2 s sr) = 1 particle flux unit (pfu).

EPS P6 and P7 proton measurements do not exhibit the diurnal variations typical of 100s of keV to multiple MeV electron fluxes at geosynchronous, including during periods when the Earth's radiation belts are significantly enhanced. This lack of electron contamination in the EPS proton channels is illustrated in Figure 1, in which the GOES-13 EPS P6 and P7 fluxes from September 2017 are plotted along with the >0.8 and >2 MeV radiation belt fluxes also observed by GOES-13 EPS. In addition, solar energetic electrons are not expected to penetrate directly to GEO due to low magnetic rigidity in their characteristic energy range. Therefore, there is no evidence that GOES EPS solar proton observations are contaminated by solar electron fluxes.

KIEL-UP • DOI: 10.38072/2748-3150/p32

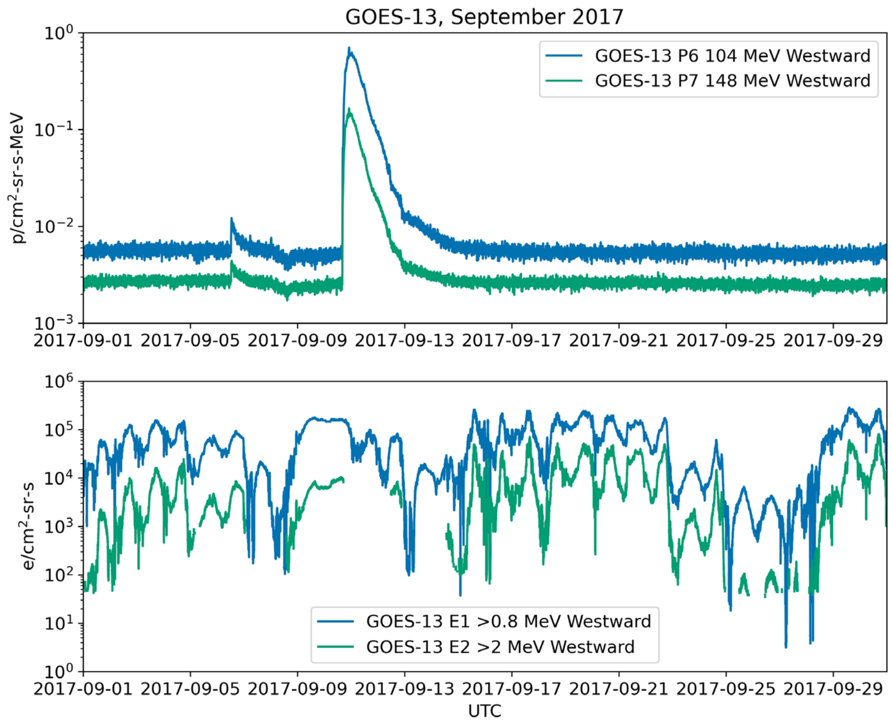

Fig. 1: GOES-13 EPS proton and electron fluxes from September 2017, illustrating the lack of electron contamination of the proton fluxes. The top panel shows the P6 and P7 channel proton fluxes observed by the westward-looking EPS. The indicated energies are from the cross-calibration by Sandberg et al. (2014). The bottom shows the >0.8 and >2 MeV radiation belt electron fluxes observed by the same instrument. The gaps in the >2 MeV fluxes correspond to periods when the observations are dominated by contamination from solar protons or when the electron fluxes are below background levels. While the EPS >2 MeV electron fluxes are always contaminated by proton fluxes from large SEP events, the converse is not true.

In addition to EPS, a High Energy Proton and Alpha Detector (HEPAD) solid-state telescope (70-degree full-angle conical FOV) measured >330 MeV protons on GOES 4-15. The GOES-4 and -5 HEPAD data were not archived, and the GOES-7 HEPAD failed on-orbit. Therefore, HEPAD data are available from GOES-6 and 8-15 (Sauer 1993; Sellers & Hanser 1996; Raukunen et al. 2020). The first GLE observed by GOES-6 was GLE 39 (February 1984), and the final GLE observed by GOES 13-15 was GLE 72 (September 2017). An enhancement above cosmic ray backgrounds in the HEPAD >700 MeV proton channel was a reliable signature of the primary component of a GLE, with some important exceptions (Thakur et al. 2016).

The HEPAD proton channels result from triple coincidences among two silicon detectors and the output of a photomultiplier tube illuminated by a fused silica Cherenkov radiator (Rinehart 1978). The nominal energies of the proton channel set are 330-420 MeV (P8), 420-510 MeV (P9), 510-700 MeV (P10), and >700 MeV (P11) (Sellers & Hanser 1996). In actuality, the response functions overlap substantially, and all of the channels have significant responses above their nominal energy range, those for P8 and P9 being due to rear entry (Raukunen et al. 2020). Signals above backgrounds in the two alpha particle channels are very rare and moreover are contaminated by proton fluxes, since protons in the tail of the distribution are mistaken for alpha particles (Blake & Kolasinski, n.d.). HEPAD was designed to reject <4 MeV electrons in-aperture and <7 MeV electrons out-of-aperture (Rinehart 1978) and was measured

KIEL-UP • DOI: 10.38072/2748-3150/p32

to have no significant response below 10 MeV (Panametrics 1980). Although HEPAD proton fluxes are susceptible to contamination by >10 MeV electrons (Blake & O'Brien 2012), observable levels of such electron fluxes are rare in geostationary orbit and can be distinguished by their characteristic diurnal variations, which are not present in >330 MeV solar proton fluxes.

Comparative plots of the onsets of GLE events from Solar Cycles 23 and 24 as observed by neutron monitors and by GOES EPS (channel P7 and >100 MeV flux) and HEPAD (channels P8, P9, P10 and P11), all at 1-minute resolution, can be found in He and Rodriguez (2018; GLEs 55-71) and in Redmon et al. (2018; GLE 72).

Accurate EPS and HEPAD calibrations have been difficult to achieve. While important work on cross-calibration and incorporation of EPS and HEPAD into models has been performed recently (Sandberg et al. 2014; Bruno 2017; Rodriguez et al. 2017; Raukunen et al. 2020; Kress et al. 2021; Hu & Semones 2022), the final word on EPS and HEPAD calibrations has yet to be written.

The flow of space environment data from GOES-13 ceased on 14 December 2017. The flow of space environment data from GOES-14 and -15 ceased on 4 March 2020.

3. New solar proton detector on GOES-16+

The first of a new series of particle detection instrument suites – the Space Environment In-Situ Suite (SEISS) – was launched on GOES-16 on November 19, 2016. Subsequently, SEISS has launched on GOES-17 (01 March 2018) and GOES-18 (01 March 2022). SEISS consists of five instruments, four of which measure solar energetic particle (SEP) fluxes (Dichter et al. 2015; Kress et al. 2020). These instruments represent the first completely new designs of GOES SEP detectors directed by NOAA since the 1970's. The primary SEP instrument is the Solar and Galactic Proton Sensor (SGPS). Each satellite carries two SGPS instruments, one looking east and one looking west. The westward observations of solar protons are attenuated much less by geomagnetic cutoffs than the eastward observations (Rodriguez et al. 2010; Kress et al. 2013). SGPS observes 1-500 MeV solar proton fluxes in 13 differential channels and integral fluxes in a >500 MeV channel, and 1-224 MeV/nucleon alpha particle fluxes in 12 differential channels. From 1 to 12 MeV, its energy range overlaps the 4 highest energy channels of the proton telescopes of the Magnetospheric Particle Sensor - High Energy (MPS-HI). The Energetic Heavy Ion Sensor (EHIS) observes heavy ion fluxes in 5 differential channels spanning energy ranges that vary from 18-335 MeV/nucleon for carbon to 39-897 MeV/nucleon for copper. In addition, EHIS observes H (11-239 MeV) and He (11-154 MeV/nucleon) ion fluxes.

A more detailed description of the SGPS instrument and data, including the proton energy channels and their geometric factors, is provided by Kress et al. (2021). In brief, each SGPS consists of three passively-shielded solid state telescopes, each of which covers a different part of the 1-500 MeV energy range. The three telescopes have 60, 60 and 90 degree conical fields-of-view. The >500 MeV proton channel has a much larger geometric factor (2.5 cm^2 sr; Kress et al. 2021) than the HEPAD channels in a similar energy range (~0.6 cm^2 sr; Raukunen et al. 2020). Kress et al. (2021) include a comprehensive evaluation of the GOES-16 proton fluxes from the SEP event commencing on 10 September 2017, which included the primary component of GLE 72. Based on cross-calibrations during this SEP event, the SGPS fluxes above 100 MeV are about a factor of two greater than the equivalent EPS fluxes when the effective EPS

KIEL-UP • DOI: 10.38072/2748-3150/p32

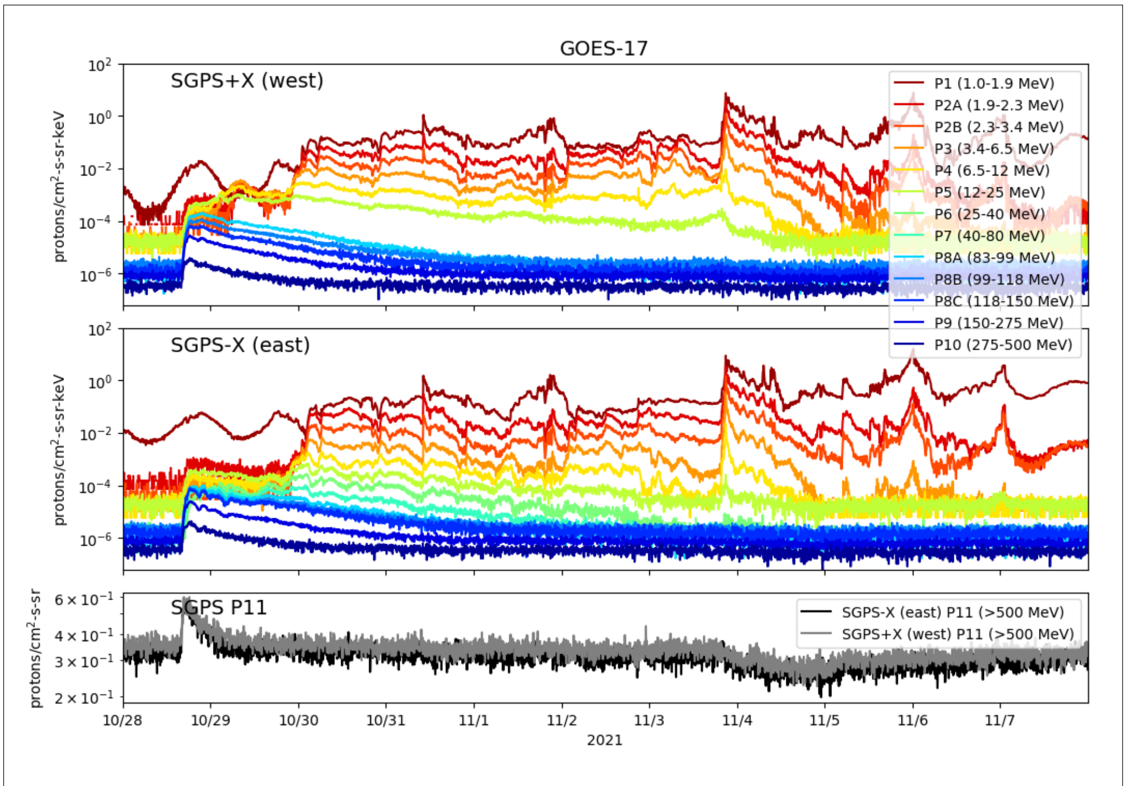

Fig. 2: GOES-17 SGPS proton fluxes from 28 October through 7 November 2021, showing the GLE 73 SEP event. The top panel shows the 1-500 MeV differential fluxes observed by the eastward-looking SGPS. The middle panel is a similar plot of the observations by the westward-looking SGPS. The bottom panel shows the >500 MeV fluxes from both the eastward and westward SGPSs.

energies derived by Sandberg et al. (2014) are used in the analysis. These effective EPS energies in turn were derived from cross-calibrations with IMP-8 observations. SWPC's >100 MeV solar proton alerts are issued based on integral fluxes derived using a new algorithm from the six channels of the third telescope of the westward-looking SGPS (Rodriguez et al. 2017; Kress et al. 2021). The EPS >100 MeV proton flux had an upper integration limit of 500 MeV, and in the absence of a SEP event, the backgrounds were residual noise from background subtractions. In contrast, the SGPS >100 MeV proton flux includes the >500 MeV P11 channel flux in the sum, and in the absence of a SEP event, the backgrounds represent the calibrated >500 MeV GCR proton flux. SGPS differential and integral fluxes are available in 1-minute and 5-minute averages.

The first GLE event of Solar Cycle 25, commencing on 28 October 2021, was observed by the GOES-16 and -17 SGPS instruments. The GOES-17 SGPS time series are shown in Figure 2. The lower energy channels from the eastward-facing sensor exhibit more fluctuations than the fluxes from the westward-facing sensor, due to time-variations in the geomagnetic cutoffs. The P11 >500 MeV channel is sensitive to the primaries of GLE 73 and to the Forbush decrease (Forbush 1937) in galactic cosmic ray (GCR) fluxes that commenced late on 3 November following the arrival of a solar wind shock at Earth.

The SGPS differential channels were designed and calibrated to observe SEP events, whose spectra decrease with energy. In the presence of a GCR spectrum, which is flat or increasing with energy over

KIEL-UP • DOI: 10.38072/2748-3150/p32

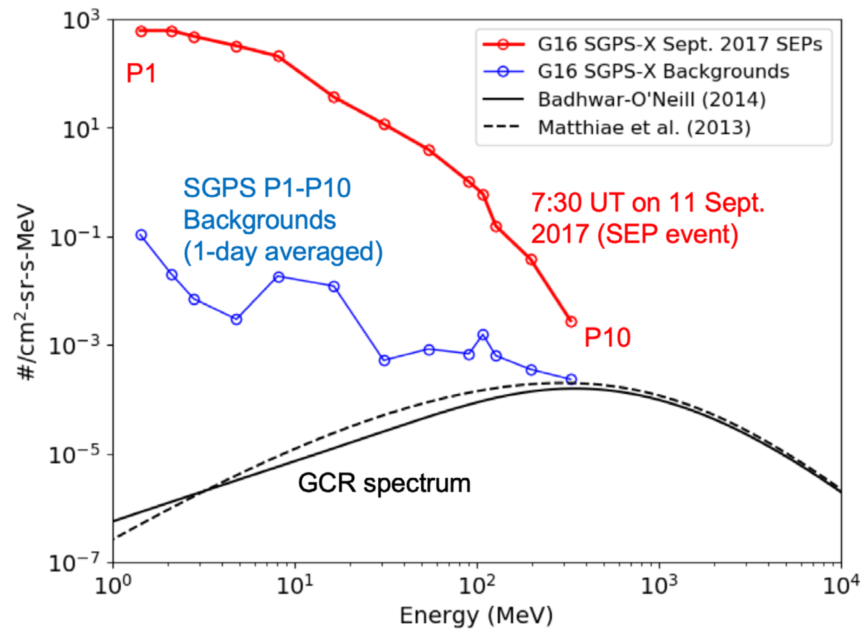

Fig. 3: GOES-16 SGPS background fluxes (blue curve), a GOES-16 SGPS solar proton spectrum from 11 September 2017, 0730 UT (red curve), and GCR model spectra from the Matthiä et al. (2013) and O'Neill et al. (2015) models (black curves). The P10 channel provides a calibrated measure of differential GCR proton fluxes in the absence of solar proton fluxes.

the SGPS energy range, the backgrounds in channels P3-P9 (3.4-275 MeV) are up to several orders of magnitude greater than the GCR flux levels at those energies, due to their sensitivity to higher-energy protons (Figure 3). In the absence of a large SEP event, the fluxes in SGPS channels P1 and P2 are dominated by trapped magnetospheric protons, which exhibit similar temporal variations to radiation belt electrons, and the SGPS P10 fluxes are within a factor of two of fluxes predicted by the Matthiä et al. (2013) and Badhwar-O'Neill 2014 (O'Neill et al. 2015) GCR models. Since the P10 energy band (276-404 MeV) bounds the GCR spectrum peak, it provides a calibrated measure of GCR flux during quiet solar conditions. SGPS channels P10 and P11 thus provide reliable GCR differential and integral proton fluxes, respectively, in their energy ranges.

The GLE 73 event was an unusual event in that the typical decreasing power law spectrum was not observed until 30 October 2021. On 28 October, the 3.4-23 MeV fluxes were sufficiently low that they were dominated by contamination from >60 MeV protons, to which the Telescope 1 channels are sensitive (Kress et al. 2021). In spectra from 28 October (18 UT), the P1 and P2A,B fluxes represent the high-energy tail of the trapped magnetospheric proton population, while P3, P4 and P5 are dominated by their >60 MeV responses (Figure 4). These low-energy SGPS fluxes should be treated with caution in the presence of a hard proton energy spectrum until a correction is put in place for this contamination.

KIEL-UP • DOI: 10.38072/2748-3150/p32

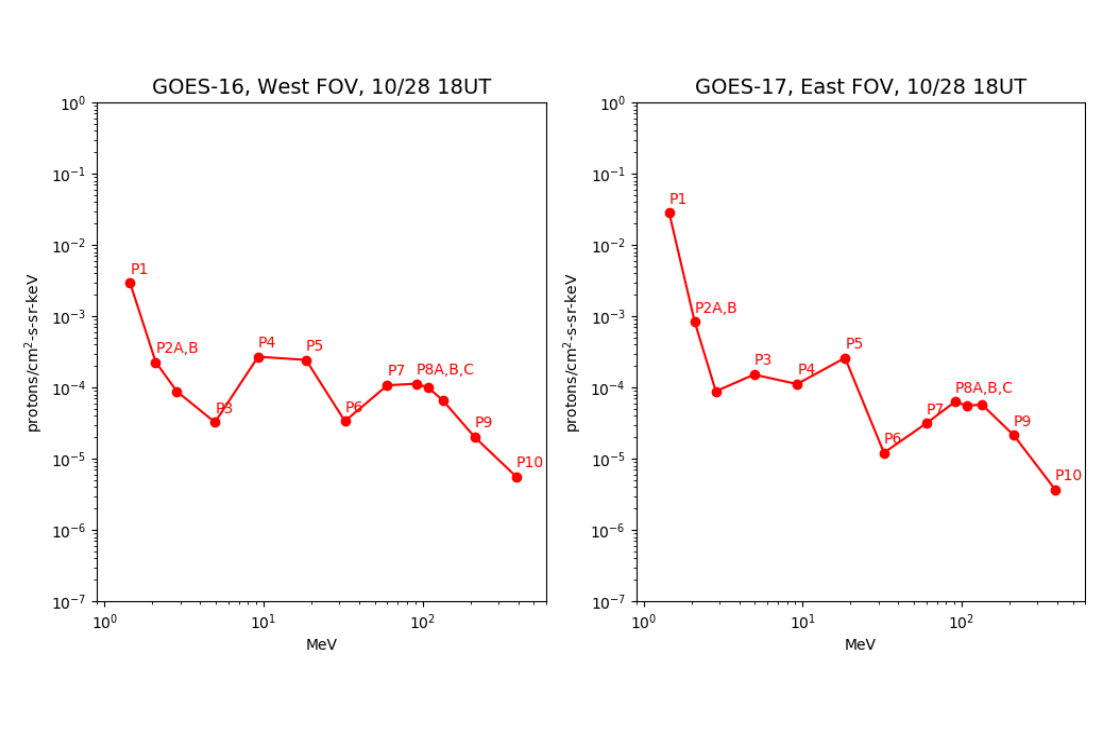

Fig. 4: SGPS proton differential number flux energy spectra from 28 October 2021, 1800 UT. (Left) Spectrum from the westward-looking SGPS on GOES-16. (Right) Spectrum from the eastward-looking SGPS on GOES-17. P3, P4, and P5 show evidence of contamination by >60 MeV protons.

4. NOAA and GLE Alert Plus alerts of GLEs 72 and 73

The NOAA SWPC and GLE Alert Plus SEP detection protocols are qualitatively different and produce different results. The NOAA method has a human forecaster in the loop. The forecaster observes 5-minute real-time averages of >10 MeV and >100 MeV proton fluxes from a single GOES satellite designated the primary satellite for space weather alerts. After three consecutive 5-minute flux averages are above a fixed threshold, an alert is issued. The first >10 MeV threshold is 10 pfu. The sole >100 MeV threshold is 1 pfu. This protocol prevents false alerts but introduces at least a 15-minute delay from the onset of a SEP event.

The GLE Alert Plus alert relies on real-time 1-minute data from multiple stations in the Neutron Monitor Database (NMDB). Following the method of Kuwabara et al. (2006), a moving threshold that is the sum of a running average and the scaled standard deviation of the count rates is calculated for each neutron monitor (NM) station (Souvatzoglou et al. 2014; Mavromichalaki et al. 2018). Depending on the value of this moving threshold, each station is at one of four alert levels (quiet, watch, warning, and alert). For a general alert to be issued, at least three stations must be in alert mode. The alert is issued automatically, and the alert status of each station is provided graphically.

GLE Alert Plus first successfully issued a real-time alert for GLE 72, whose onset was on 10 September 2017 (Mavromichalaki et al. 2018). GLE Alert Plus issued the first NM station alert (Fort Smith) at 1618 UT, and the general alert based on four stations (Kerguelen, Inuvik, South Pole Bares, Thule) was issued at 1658 UT. The

KIEL-UP • DOI: 10.38072/2748-3150/p32

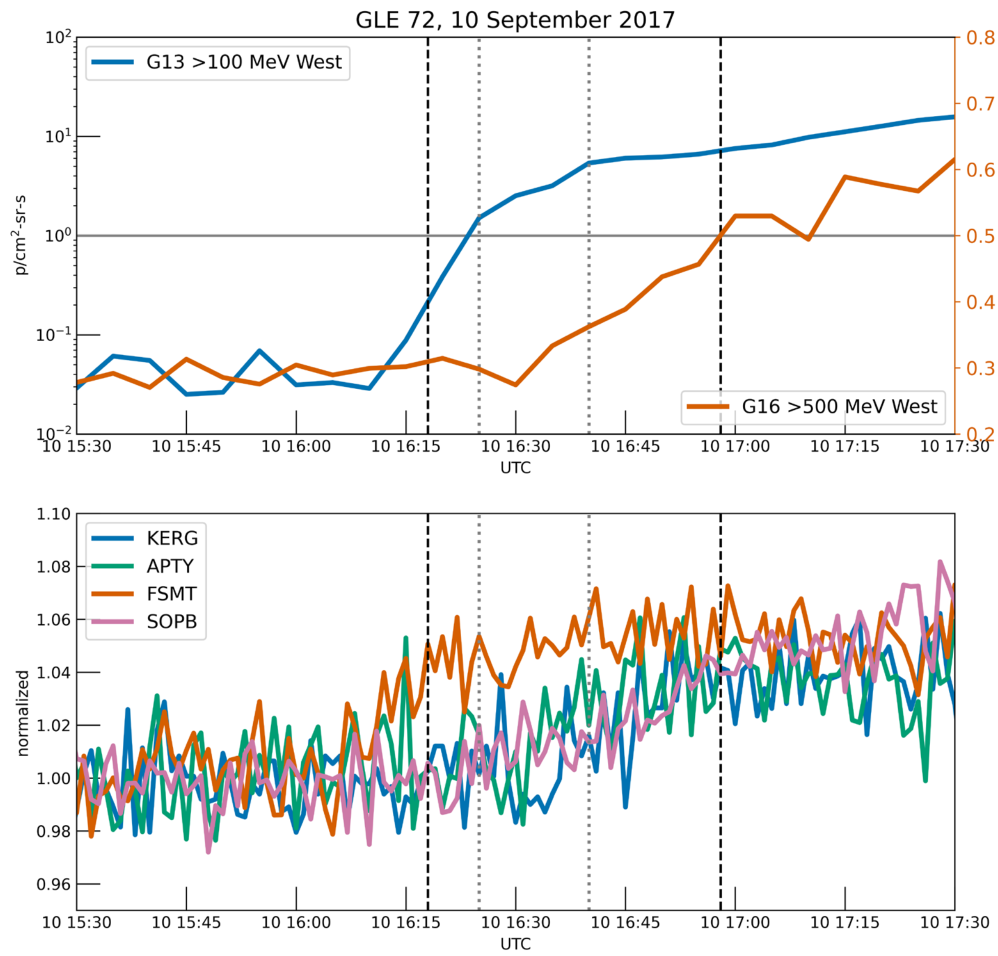

Fig. 5: The onset of GLE 72 as observed (top) by GOES-13 EPS >100 MeV and GOES-16 SGPS >500 MeV fluxes and (bottom) by the Kerguelen, Apatity, Fort Smith, and South Pole Bare neutron monitors. The GOES data are shown in integral flux units, with different scales for the two observations due to the much smaller increase in the >500 MeV fluxes. The NM data are normalized to the pre-event levels. The first vertical dashed line indicates the first NM station alert (Fort Smith) at 1618 UT. The first vertical dotted line indicates when the GOES-13 >100 MeV flux crossed the 1 pfu threshold (1625 UT). The second vertical dotted line indicates when SWPC issued the >100 MeV alert (1640 UT). The second vertical dashed line indicates when GLE Alert Plus issued the general alert (1658 UT).

GOES-13 >100 MeV flux crossed the 1-pfu threshold at 1625 UT, and SWPC issued the >100 MeV alert at 1640 UT. Therefore, though the first NM station alert preceded the NOAA alert by 7 minutes, the NOAA alert led the GLE Alert Plus general alert by 18 minutes (Figure 5). The GOES-13 >100 MeV proton flux rose above background noise similarly to the Fort Smith NM, while the rise of the GOES-16 >500 MeV solar proton flux above the GCR level was similar to some of the other NM stations like Apatity and Kerguelen. As discussed in connection with Figure 1, the early onset of the GOES-13 >100 MeV proton fluxes was not due to electron contamination. The count rates from the EPS P7 channels on GOES-14 and -15 rose less rapidly than the GOES-13 P7 count rates, from which the >100 MeV fluxes used in the SWPC alert were derived (Redmon et al. 2018). This difference among the three GOES EPS observations may indicate a longitudinal variation in geostationary orbit.

KIEL-UP • DOI: 10.38072/2748-3150/p32

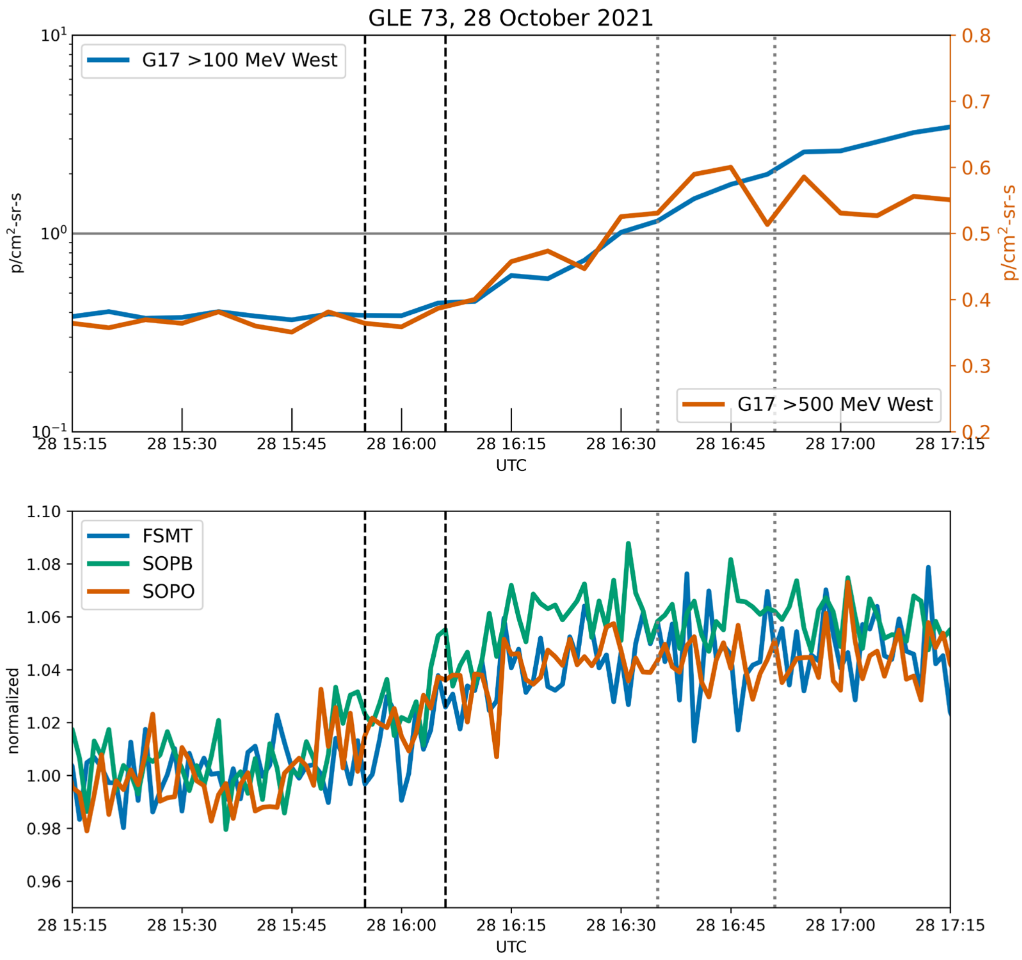

Fig. 6: The onset of GLE 73 as observed (top) by GOES-17 SGPS >100 MeV and >500 MeV proton fluxes and (bottom) by the Fort Smith, South Pole and South Pole Bares neutron monitors. The GOES data are shown in integral flux units, with different scales for the two observations due to the much smaller increase in the >500 MeV fluxes. The NM data are normalized to the pre-event levels. The first vertical dashed line indicates the first NM station alert (South Pole Bares) at 1555 UT. The second vertical dashed line indicates when GLE Alert+ issued the general alert (1606 UT). The first vertical dotted line indicates when the GOES-16 >100 MeV flux crossed the 1 pfu threshold (1635 UT). The second vertical dotted line indicates when SWPC issued the >100 MeV alert (1651 UT).

The onset of GLE 73 was on 28 October 2021. GLE Alert++ issued the first NM station alert (South Pole Bares) at 1555 UT, and the general alert based on 3 stations (Fort Smith, South Pole and South Pole Bares) was issued at 1606 UT. The GOES-16 >100 MeV flux crossed the 1-pfu threshold at 1635 UT, and SWPC issued the >100 MeV alert at 1651 UT, 45 minutes after the GLE Alert++ general alert (Figure 6). In this case, the GOES flux increases visibly occurred about 15 minutes later than the NM count rate increases, and the use of a fixed threshold based on a single satellite, rather than a moving threshold operating on data from two satellites, delayed the GOES alerts further.

5. Discussion

In a study of the onsets of GLEs 55-71 that applied a moving threshold detection method similar to that of Kuwabara et al. (2006) to 1-minute NM and GOES data, He and Rodriguez (2018) found that the median difference in the event detection times between NM and GOES was 0 minutes, with the 10th, 25th, 75th, and 90th percentiles of the differences (GOES minus NMs) being -7.2, -1.5, +2.5, and +4.2 minutes, respectively. The detection thresholds were set to avoid false alarms using a three-station coincidence for NM data and a two-satellite coincidence for GOES data. Using the same algorithm, GLE 72 was detected by some GOES 13-15 HEPAD channels within two minutes of the Fort Smith station alert (1618 UT) issued by GLE Alert Plus (Redmon et al. 2018). These differences between NMs and GOES may be due partly to energy dependencies, anisotropies and geomagnetic effects, and partly to different noise and event-to-background levels in different instruments. A deeper understanding of the causes of these differences should be pursued.

Regardless, a practical alert system should take advantage of these differences to reduce alert delays. As suggested by He and Rodriguez (2018), an alert system should be developed that relies on real-time 1-minute data from the NMDB network and from both operational GOES satellites. The >100 MeV and >500 MeV fluxes from both SGPS instruments on each satellite should be used in such an alert system, although not all GOES solar proton enhancements in these energy ranges correspond to GLEs (Thakur et al. 2016). The moving threshold method originally developed by Kuwabara et al. (2006) and implemented successfully in GLE Alert Plus (Souvatzoglou et al. 2014; Mavromichalaki et al. 2018) should be applied to both the NM and the GOES data.

6. Summary

The long series of GLE event observations by the GOES Energetic Particle Sensors (EPS) and High Energy Proton and Alpha Detectors (HEPAD) ended with GLE 72 in September 2017. That GLE was also the first observed by the series of new Solar and Galactic Proton Sensors (SGPS). To date, SGPS units on two GOES satellites have observed the primary components of GLEs 72 and 73. The GOES-based >100 MeV alert issued by NOAA at the onset of GLE 72 preceded the general alert issued by the NMDB-based GLE Alert Plus system, while the situation was reversed for GLE 73. Understanding the causes of such differences requires an investigation into the energy-, angular and propagation differences among GLE events that accounts for different instrument sensitivities and noise levels. Regardless of the causes of these differences, alert systems should be able to reduce alert delays by relying on observations by the NMDB network and the two operational GOES satellites.

Acknowledgements

We acknowledge the NMDB database (www.nmdb.eu) founded under the European Union's FP7 programme (contract no. 213 007), and the PIs of individual neutron monitors. This research was supported in part by NOAA cooperative agreement NA17OAR432010. Support was also provided by the Air Force Office of Sponsored Research (AFOSR) under grant FA9550-20-1-0339. The historical GOES-15

and earlier EPS and HEPAD data are available at https://www.ncei.noaa.gov/data/goes-space-environment-monitor/. The reprocessed pre-operational GOES-16 SGPS solar proton data from GLE 72 are available at https://www.ngdc.noaa.gov/stp/space-weather/satellite-data/satellite-systems/goesr/solar_proton_events/sgps_sep2017_event_data/. The operational GOES-16+ SGPS data are available in real time in JSON format at https://services.swpc.noaa.gov/json/goes/ and retrospectively in daily netCDF files at https://www.ncei.noaa.gov/products/goes-r-space-environment-in-situ.

References

Blake, J. B., and Kolasinski, W. A. (no date). Preliminary evaluation of the NOAA High Energy Proton and Alpha-Particle Detector performance, https://www.ncei.noaa.gov/data/poes-metop-space-environment-monitor/doc/reports/POES_SEM1_HEPAD_Blake-Kolasinski.pdf (last accessed September 19, 2023).

Blake, J. B. and O'Brien, T. P. 2012. On the relativistic electron event in early April 2010. 39th COSPAR Scientific Assembly, paper D.3.4.

Bruno A. 2017, Calibration of the GOES 13/15 high-energy proton detectors based on the PAMELA solar energetic particle observations. *Space Weather,* 15, 1191–1202, https://doi.org/10.1002/2017SW001672.

Dichter, B. K., Galica, G. E., McGarity, J. O., Tsui, S., Golightly, M. J., Lopate, C., and Connell, J. J. 2015, Specification design and calibration of the space weather suite of instruments on the NOAA GOES-R program spacecraft. IEEE Transactions on Nuclear Science, 62(6), 2776–2783, https://doi.org/10.1109/TNS.2015.2477997

He, J., and Rodriguez, J. V. 2018, Onsets of solar proton events in satellite and ground level observations: A comparison. Space Weather, 16, 245–260, https://doi.org/10.1002/2017SW001743

Hu, S., and Semones, E. 2022. Calibration of the GOES 6–16 high-energy proton detectors based on modelling of ground level enhancement energy spectra. J. Space Weather Space Clim., 12, 5, https://doi.org/10.1051/swsc/2022003

Kress, B. T., Rodriguez, J. V., Mazur, J. E., & Engel, M. 2013, Modeling solar proton access to geostationary spacecraft with geomagnetic cutoffs. Advances in Space Research, 52, 1939–1948, https://doi.org/10.1016/j.asr.2013.08.019

Kress, B. T., Rodriguez, J. V. and Onsager, T.G. 2020, The GOES-R space environment in situ suite (SEISS): Measurement of energetic particles in geospace. *The GOESR Series*, Elsevier, 243-250, https://doi.org/10.1016/B978-0-12-814327-8.00020-2

Kress, B. T., Rodriguez, J. V., Boudouridis, A., Onsager, T. G., Dichter, B. K., Galica, G. E., and Tsui, S. 2021, Observations from NOAA's newest solar proton sensor. Space Weather, 19, e2021SW002750, https://doi.org/10.1029/2021SW002750

Kuwabara, T., Bieber, J. W., Clem, J., Evenson, P., and Pyle, R. 2006, Development of a ground level enhancement alarm system based upon neutron monitors, Space Weather, 4, S10001, https://doi.org/10.1029/2006SW000223

Matthiä, D., Berger, T., Mrigakshi, A.I. and Reitz, G. 2013, A ready-to-use galactic cosmic ray model. Advances in Space Research, 51(3), 329-338, https://doi.org/10.1016/j.asr.2012.09.022

Mavromichalaki, H., Gerontidou, M., Paschalis, P., Paouris, E., Tezari, A., Sgouropoulos, C., et al. 2018, Real-time detection of the ground level enhancement on 10 September 2017 by A.Ne.Mo.S.: System report. Space Weather, 16, 1797–1805, https://doi.org/10.1029/2018SW001992

Mavromichalaki, H., Paschalis, P., Gerontidou, M., Papailiou, M.C., Paouris, E., Tezari, A., Lingri, D., Livada, M., Stassinakis, A.N., Crosby, N. and Dierckxsens, M. 2022, The updated version of the A. Ne. Mo. S. GLE Alert System: The case of the ground-level enhancement GLE73 on 28 October 2021. Universe, 8(7), 378, https://doi.org/10.3390/universe8070378

O'Neill, P. M., Golge, S., and Slaba, T. C. 2015, Badhwar-O'Neill 2014 galactic cosmic ray flux model description, NASA TP-2015-218569

Panametrics 1980, March 1980 HEPAD tests. SN6 and SN8 preliminary data analysis. PANA-SEM-1. https://www.ngdc.noaa.gov/stp/satellite/goes/doc/goes_nop/PANA-SEM-1_HEPAD_18Jul1980.pdf (last accessed September 14, 2023)

Raukunen, O., Paassilta, M., Vainio, R., Rodriguez, J.V., Eronen, T., Crosby, N., Dierckxsens, M., Jiggens, P., Heynderickx, D. and Sandberg, I. 2020, Very high energy proton peak flux model. Journal of Space Weather and Space Climate, 10, 24, https://doi.org/10.1051/swsc/2020024

Redmon, R. J., Seaton, D. B., Steenburgh, R., He, J., & Rodriguez, J. V. 2018, September 2017's geoeffective space weather and impacts to Caribbean radio communications during hurricane response. Space Weather, 16, 1190–1201, https://doi.org/10.1029/2018SW001897

KIEL-UP • DOI: 10.38072/2748-3150/p32

Rinehart, M. C. 1978, Cerenkov counter for spacecraft application. Nuclear Instruments and Methods, 154(2), 303-316, https://doi.org/10.1016/0029-554X(78)90414-7

Rodriguez, J. V., Onsager, T. G., & Mazur, J. E. 2010, The east-west effect in solar proton flux measurements in geostationary orbit: A new GOES capability. Geophysical Research Letters, 37, L07109, https://doi.org/10.1029/2010GL042531

Rodriguez, J. V., Sandberg, I., Mewaldt, R. A., Daglis, I. A., & Jiggens, P. 2017, Validation of the effect of cross-calibrated GOES solar proton effective energies on derived integral fluxes by comparison with STEREO observations. Space Weather, 15, 290–309, https://doi.org/10.1002/2016SW001533

Sandberg, I., Jiggens, P., Heynderickx, D., & Daglis, I. A. 2014, Cross calibration of NOAA GOES solar proton detectors using corrected NASA IMP-8/GME data. Geophysical Research Letters, 41, 4435–4441, https://doi.org/10.1002/2014GL060469

Sauer H. H. 1993, GOES observations of energetic protons to E>685 MeV: Description and data comparison. In: Proceedings of the 23rd International Cosmic Ray Conference, Leahy DA, Hicks RB, Venkatesan D (Eds.), Vol. 3, Calgary, Canada, 250-253. https://adsabs.harvard.edu/full/record/seri/ICRC./0023/1993ICRC....3..250S.html (last accessed September 14, 2023)

Souvatzoglou, G., Papaioannou, A., Mavromichalaki, H., Dimitroulakos, J., & Sarlanis, C. (2014). Optimizing the real-time ground level enhancement alert system based on neutron monitor measurements: Introducing GLE Alert Plus. Space Weather, 12, 633–649, https://doi.org/10.1002/2014SW001102

Thakur, N., Gopalswamy, N., Mäkelä, P., Akiyama, S., Yashiro, S. and Xie, H., 2016. Two exceptions in the large SEP events of solar cycles 23 and 24. *Solar Physics*, *291*(2), 513-530, https://doi.org/10.1007/s11207-015-0830-9

Open Access